J Mater Sci (2010) 45:6126–6138
DOI 10.1007/s10853-010-4699-6

Synergy in carbon black-filled natural rubber nanocomposites. Part I: Mechanical, dynamic mechanical properties, and morphology

Mithun Bhattacharya · Anil K. Bhowmick

Received: 31 January 2010 / Accepted: 7 June 2010 / Published online: 16 June 2010

Abstract Natural rubber (NR)/nanoclay and NR/carbon nanofiber (CNF) nanocomposites were consolidated with different loadings and grades of carbon blacks (CBs) to obtain ternary nanocomposites. It was observed that the mechanical and dynamic mechanical properties of these nanocomposites were much better compared with those of either NR/clay or NR/CNF nanocomposites or the NR/black control microcomposite. Thus, not only the grueling and at times conflicting property requirements of modern day applications were met, but also the tendency of saturation of property enhancements at high loadings could be mitigated. These nanocomposites exhibited 18% increment in tear strength, 40% in modulus at 300% elongation, and 326% in room temperature storage modulus, over the control microcomposite. Viscous loss properties were influenced favorably, as well. This indicated the presence of a much sought after synergy between CB and nanofillers. Transmission electron micrographs of the nanocomposites showed that CB formed "nano-blocks" of reinforcement—close association of nanofiller and black—driven by zeta potential differences between the black and the nanofillers. This unique ternary architectural base, with the space between nanofillers (clay/fiber) occupied by small CB aggregates forming networks or "nano-channels", accounted for the synergistic improvements.

M. Bhattacharya · A. K. Bhowmick
Rubber Technology Center, Indian Institute of Technology, Kharagpur 721302, India
e-mail: bhatt.mithun@gmail.com

A. K. Bhowmick (✉)
Indian Institute of Technology, Patna 800013, India
e-mail: anilkb@rtc.iitkgp.ernet.in; director@iitp.ac.in

Introduction

Nanomaterials and polymer nanocomposites have been growth drivers in the field of advanced materials research over the past decade. Dispersing nanoparticles in polymer matrices has been a preferred and widely used means of improving the properties of polymers. Inherent properties of nanofillers determine enhancement in material properties by virtue of extended interface region. Nanocomposites exhibit properties very different from their bulk conventional composite counterparts [1, 2] due to high surface-to-volume ratio [3] and nanometer scale dispersion of the reinforcing agents. Amongst the different nanofillers prevailing in modern research, layered silicates and carbon nanotubes have received utmost attention. The pioneering research of the Toyota group [4, 5] introduced polyamide organoclay nanocomposites. Polymer-layered silicate nanocomposites have ever since grabbed the attention of researchers worldwide [6–9]. On the other hand, ever since their discovery in 1991 by Iijima [10], carbon nanotubes (CNTs) have inspired interest for being used as a filler in polymer composite systems to obtain ultra-light structural materials with enhanced mechanical, electrical, thermal, and optical characteristics [11, 12] primarily due to their remarkable physical and mechanical properties. Vapor-grown carbon fibers (VGCFs), a species similar to multi-walled CNTs, comprise graphitic networks in concentric cylinders encircling a hollow nanotube core [13–15]. Since VGCFs have a much lower production cost than CNTs and are readily available in bulk quantities, VGCFs are commercially attractive [16]. Although they have sparingly been used in rubber, our previous research has highlighted the marked enhancements of rubber nanocomposite properties, especially the tear strength, on utilization of VGCFs [17, 18].

However, the biggest problem plaguing polymer nanocomposites is the difficulty of dispersion at higher loadings (typically above 6–8 phr), because beyond such critical loading most of the properties dip due to agglomeration. Thus, only a well-informed and judicious choice of filler and its incorporation technique can produce materials suitable for the most rigorous and advanced applications.

In order for rubbers to have real-life applications, several ingredients have to be incorporated into them, the most prime among them being the filler. The main aim behind addition of filler is to improve certain properties, to reinforce the matrix and to cheapen the compound. The reinforcement of rubbers is expressed by enhancement of the modulus, failure properties (tensile and tear strength) and abrasion resistance of the vulcanizates, and carbon black (CB) is the material of choice for attainment of these properties [19, 20]. Over the last two decades, research has focused to find complete or at least partial replacement of CB in rubber compounds and to impart multifarious properties, thereby initiating search and development of other reinforcing agents. Kaolin and precipitated silica have commonly been used as semi-reinforcing agents.

Like nanofillers, CB can induce property enhancements till a certain loading (typically up to $\sim$40 phr, depending although on the matrix), beyond which critical properties fall beyond acceptable limits. The probability of favorable interactions between two such reinforcing fillers (CB and nanofillers) can spring some synergy, and thus, it would be of interest to investigate whether such synergy can result in sustenance of property enhancements at loadings beyond which individually either of the fillers fail.

This synergistic behavior is of paramount importance in many rigorous present day applications which demand contradictory performance properties. For instance, tire compound formulators hypothetically aspire to attain radially expanding magic triangle output performance. This involves better wear resistance, wet grip, and lower rolling resistance, all at the same time. This chasm between performance and requirement may be bridged by nanomaterials in the presence of conventional fillers. The black grade and amount, in this study, were selected to impart abrasion resistance, durability, traction, cornering coefficient, and rolling resistance necessary for good performance in the targeted end use in tire tread application.

From the literature survey, we find that black-filled rubber vulcanizate properties and their dependence on size, structure, and surface activity of CB has earlier been discussed [19] and at the same time, state of the art in nanocomposites has also been widely researched [2–9, 11, 12, 17, 18]. However, till date, these fillers have been studied in relative isolation. The literature search also reveals that although a couple of reports exists on the effect of black on rubber nanocomposites (RNC) [21, 22] such studies have not been undertaken with respect to application-oriented products. Effect of nature and loading of CB on brominated poly(isobutylene-co-paramethylstyrene) (BIMS) rubber and octadecyl amine-modified montmorillonite-based nanocomposites was investigated thoroughly using X-ray diffraction technique (XRD), Fourier transform infrared spectroscopy and mechanical properties. Optimum results were obtained with the 20-phr filler loading. The addition of four parts of the modified nanoclay to 20 phr N550 CB-filled samples increased the tensile strength by 53% over the only CB-filled composites [21].

In a similar study, Jia et al. prepared clay/CB/NR composites by adding CB in a two-roll mixing mill to clay-premixed NR latex. They found that at the same total filling amount, those NR nanocomposites filled with both fillers showed enhanced mechanical properties, improved processability and gas permeability [22]. In the case of RNC, while the much improved performance over black-filled conventional composites at low filler loading is acclaimed, one generally fails to achieve the continuous property enhancements provided by CB at very high loadings.

This shortcoming along with the commercial necessity of engineering compounds to meet the demanding and at times conflicting spectrum of advanced performance properties motivates this study on the synergy in CB-containing NR nanocomposites. The study investigates the sustainability of property enhancements in the presence of usual CB loadings. Our previous publications [17, 18] have established the effect of nanofillers and their dispersion techniques on the mechanical and dynamic mechanical properties, along with the resultant morphology of the nanocomposites. The effect of black at similar low loadings has also been discussed [17, 18]. In an earlier publication [18], the effect of nanofillers, their loading and different dispersion techniques in NR nanocomposite vulcanizates had been discussed in detail. Different nanofillers like unmodified and modified montmorillonite, hectorite, laponite, silica, expanded graphite and carbon nanofibers (CNFs) were studied, and it was found that sepiolite imparts the best tensile properties, while tear strength responds best to CNF addition [18]. Various modifiers and compatibilizers such as silanes, titanates, polyethylene glycol, and epoxidised NR were used to enhance the dispersion of these two nanofillers. Filler incorporation techniques were changed to study the effect of temperature, time, and speed on polymer–nanofiller interaction and concomitant dispersion. Modification of the sepiolite with titanate improved their properties the most. On the other hand, chemical modifications did not significantly alter the properties of the CNF-filled nanocomposites, but their dispersion was found to have been enhanced on mixing the nanofibers in the Brabender at slow speed (20 rpm) for a longer period of time (20 min). This was attributed to the

availability of more time and space for polymer diffusion and adsorption on to the nanofiller surface [18]. In part I of this study, we explore the effect of type and amount of CB loading on the mechanical and dynamic mechanical properties of the nanocomposites. The implications of the viscoelastic properties at specific temperatures of these dual filler compounds on other tire properties, such as rolling resistance and wet skid resistance, have also been reported here.

We have discussed these observations in light of the changing morphology of the nanocomposites using Transmission Electron Microscopy studies, in conjunction with the comprehension of the ensuing electrostatic interactions in such ternary compounds. The effect on abrasion behavior has been discussed in a separate article (Part II).

Experimental

Materials

Natural rubber (Mooney Viscosity, ML_{1+4} at 100 °C = 60) was supplied by the Rubber Board, Kottayam, Kerala, India. The nanofillers used were organomodified nanoclay (SP) [Pangel B20 (Sepiolite clay from Tolsa S.A., Madrid, Spain)] and carbon nanofiber (F) [Pyrograf III, PR-24 (Vapour Grown Carbon Fiber from Pyrograf® Products Inc., Ohio, USA)]. Titanate modifier, Kenreact™ Lica 38J, was generously provided by Kenrich Chemicals, New Jersey, USA. Standard rubber grade zinc oxide and sulfur were procured from Merck Ltd., Mumbai, India. Stearic acid was supplied by Shreeji Fine Chemicals, Mumbai, India, and *N*-cyclohexyl-2-benzothiazyl sulfenamide (CBS) by ICI India Ltd., Chemicals Division, Mumbai, India. *N*-isopropyl-*N*′-phenyl-*p*-phenylenediamine (IPPD) was provided by Bayer Chemicals AG (presently, Lanxess), Leverkusen, Germany. Ethanol was procured from Bengal Chemicals and Pharmaceuticals Ltd., Kolkata, India. Different grades of CB [N220 (ISAF; mean size: 21 nm, BET N_2 surface area: 116 m^2/g), N330 (HAF; mean size: 30 nm, BET N_2 surface area: 83 m^2/g), and N550 (FEF; mean size: 56 nm, BET N_2 surface area: 41 m^2/g)] were supplied by Phillips Carbon Black, Durgapur, India. Process oil was procured from A. B. Enterprises, Mumbai, India.

The recipe is tabulated in Table 1 and is similar to that used for standard tire tread compound. The concentration of nanofillers was optimized in an earlier study [18]. The sample designation is presented in the form of a flow chart which also is the schematic of this study (Scheme 1). The scheme also explains the sample designation used.

For ease of correlation, the designations used in our earlier publication [18] have been retained for the base nanocomposites devoid of CB. In Scheme 1, TiNSP4 corresponds to the 4 phr sepiolite-based system that had been modified with titanate for better dispersion. BNF6, on the other hand, is the CNF-based system, wherein for enhancement of dispersion, the nanofibers were mixed in the Brabender Plasticorder at slow speed (20 rpm) for a longer period of time (20 min). Here, BNF6 is represented as NF-6, TiNSP4 is represented as NC-4, gum rubber is designated as R-0, the carbon blacks are represented as follows: N2 (for N220), N3 (for N330), and N5 (for N550). The number immediately following the '-' is the phr loading of CB. For instance, NF-6/N5-30 refers to the CNF nanocomposite (BNF6) filled with 30 phr of N550. Similarly, NC-4/N3-30 represents titanate-modified 4 phr sepiolite-loaded NR (TiNSP4) mixed with 30 phr of N330. The control is represented as R-0/N3-50, suggesting that it is the rubber compound devoid of either nanoclay/nanofiber (0) filled with 50 phr of N330.

The basic recipe was kept common for all the systems. There was no variation in the loading of anti-oxidant, curatives, and cure accelerators.

Table 1 Rubber formulation and order of mixing

Order of mixing	Ingredient	Loading in phr
1	Rubber	100.0
2	Nanoclay/nanofiber	4.0/6.0
3	Titanate	0.4/0.0[a]
4	Zinc oxide	5.0
5	Stearic acid	2.0
6	IPPD	1.0
7	Carbon black	50.0
8	Oil	5.0
9	CBS	0.8
10	Sulfur	2.0

[a] Nanofiber filled systems were process modified and did not contain titanate as modifier

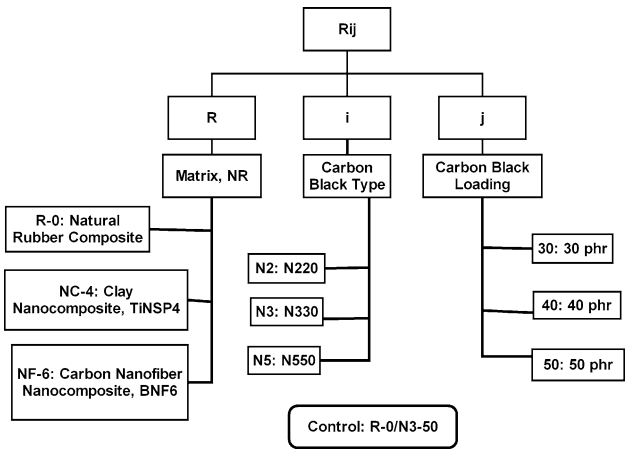

Scheme 1 Sample designation and the schematic of the study

Preparation of nanocomposites

In accordance with the observations recorded in our earlier communication [18], chemical modification of sepiolite was done with Kenreact^{TM} Lica 38J (10% of filler weight), while CNFs were mixed at 20 rpm for 12 min [18]. The modified nanofillers were initially mixed with the rubber followed by the addition of the remaining compounding ingredients, except the curative package, in accordance with the standard sequence in a Brabender Plasticorder (PLE 330) at 80 °C at 60 rpm. Table 1 not only contains the recipe of all the dual filler systems, but also highlights the order of mixing of each ingredient. Since this study intends to address the demands of real-life applications, black-filled systems were formulated in accordance with common commercial tire formulation. Black was loaded in two installments to minimize the heat generation and thus optimize the dispersion. After incorporation of black, the masterbatch was mixed for 3 min in a Brabender Plasticorder and then dumped. The curatives were finally added to the resulting masterbatch in a two-roll mill (Schwabenthan, Berlin, Germany).

Cure behavior

The tensile slabs were prepared by curing till optimum cure time at 150 °C in a David-Bridge hydraulic press (supplied by Castleton, Rocchdle, England) at a pressure of 5 MPa. The optimum cure time was obtained from a Monsanto Oscillating Disc Rheometer (ODR-100s) in accordance with ASTM D2084-93. The specimens were conditioned at room temperature for 16 h before carrying out the testing.

Tensile properties

Tensile, tear and hysteresis specimens were punched out from the molded sheets using ASTM Die-C. The tests were carried out in a Universal Testing Machine (Zwick Roell Z010, Ulm, Germany) at a cross-head speed of 500 mm/min at 25 ± 2 °C. Tensile and tear tests were carried out as per the ASTM D 412-98 and ASTM D 624-99 methods, respectively. The average of three tests has been reported here. The standard deviations for modulus at 300% elongation, tensile strength, elongation at break (EAB), and tear strength are ±0.3, ±0.6, ±7.0, and ±1.0 units, respectively.

The hysteresis loss ratio is defined as

$$(H_y)_r = (W_1 - W_2)/W_1 \quad (1)$$

where H_y, W_1, and W_2 are hysteresis loss, work performed during forward deformation, and work done during reverse deformation, respectively. Hysteresis test was performed till 200% elongation, and the Hysteresis Loss Ratio (HLR) was reported for the first cycle only.

Heat buildup (HBU)

A simple three-piece, six-cavity mold was utilized in making cylindrical rubber specimens, having diameter of 17.8 mm and height of 25 mm in accordance with ASTM D 623-93 for the Goodrich Flexometer test. Samples were cured under pressure in the David-Bridge hydraulic press. The samples were allowed to equilibrate at 50 °C for 20 min before hammering them at 1800 revolution per minute (rpm) with each stroke length of 4.45 mm. The average of three tests has been reported here. The standard deviation in HBU was found to be ±0.2 °C.

Dynamic mechanical thermal analysis (DMTA)

The dynamic mechanical spectra of the gum and RNCs were obtained using a DMTA IV (Rheometric Scientific, NJ, USA) dynamic mechanical thermal analyzer. The sample specimens were analyzed in tensile mode at a constant frequency of 1 Hz, a strain of 0.01%, over a temperature range from −90 to 80 °C, and at a heating rate of 2 °C/min. The data were analyzed by RSI Orchestrator application software. Storage modulus (E'), loss modulus (E''), and loss tangent (tan δ) were measured as function of temperature for all the samples under identical conditions. The temperature corresponding to the peak in tan δ versus temperature plot was taken as the glass–rubber transition temperature (T_g). The T_g has been reported along with the tan δ values at T_g, 0 and 60 °C. The latter two correspond to the wet skid resistance and the rolling resistance, respectively, of rubber compounds engaged in tire applications.

Transmission electron microscopy

The nanocomposite samples for Transmission electron microscopy (TEM) analysis were prepared by ultra cryo-microtomy using Leica Ultracut UCT, at around 30 °C below the glass transition temperature, T_g, of the compounds. Freshly cut glass knives with cutting edge of 45° were used to get the cryosections of 50-nm thickness. JEOL-2100 electron microscope (Tokyo, Japan) having LaB_6 filament and operating at an accelerating voltage of 200 kV was utilized to obtain the bright field images of the cryo-microtomed samples.

Results and discussion

Effect of CB on nanocomposites

In this section, the effects of CB on properties of both the gum compound and the nanocomposites have been studied

by using HAF (N330) at 50 phr loading. The black type and loading in the formulation was decided with an eye on application in tires. Toward this end, two different nanofillers have been utilized—nanoclay (NC-4 series) and carbon nanofiber (NF-6 series)—as shown in Scheme 1. The values of the modulus at 300%, tensile strength (TS), elongation at break (EAB), tear strength, HLR, and HBU for the different systems are shown in Table 2. The 50 phr HAF-filled NR control composite (designated as R-0/N3-50) shows modulus at 300% elongation of 9.19 MPa, tensile strength (TS) of 22.05 MPa, and tear strength (TR) of 46.9 N/mm, respectively. These values amount to significant increase of modulus at 300% elongation and tear strength over not only the gum, but also the base nanocomposites devoid of CB (cf. Sl. Nos. 4 Vs 2 and 3). The corresponding increments of modulus and tear strength over the nanocomposites devoid of CB are in the order of 300 and 50%, respectively. These are the minimum increments over sl. nos. 2 (TiNSP4) and 3 (BNF6) reported here (Table 2).

On introduction of black into the nanocomposites, the nanoclay-filled sample (NC-4/N3-50) registers modulus at 300% elongation of 12.15 MPa, tensile strength of 25.15 MPa and tear strength of 55.4 N/mm. These values correspond to around 32% increment in modulus at 300% elongation and 18% in tear strength, over the only black-filled microcomposite. Similarly, NF-6/N3-50 shows 16% increase in tear strength and 40% enhancement of the modulus at 300% elongation over R-0/N3-50. It must be mentioned here that 50 phr is the optimum CB loading in such compositions because properties saturate beyond this point. However, here in the presence of dual filler systems, increments are registered even above and beyond such levels, which indeed is a significant development. In the case of these compounds containing nanofiller, the concomitant increase in HLR by more than 20% contributes to the rise in tear strength, as the excess energy is required to overcome the hysteretic barrier for tear initiation [18]. HBU exhibits a mere unit degree increase over R-0/N3-50. When compared against the nanocomposites devoid of CB (TiNSP4 and BNF6), remarkable increments are observed. In the case of clay-filled sample, 53% enhancement in tear strength and 282% in the modulus at 300% elongation are observed. The corresponding increments for the nanofiber-filled compounds are 51 and 304%, respectively.

These results illustrate that even in the presence of very high loading of CB, the nano-filled composites retain the influence of the nanofiller. The HLR is found to increase because of increment in filler–filler frictional interactions with decrease in interparticle distance. The enhanced performance has been explained later with the help of morphological insights, which reflect the formation of nanoblocks from the close association of the nanofiller and the CB moieties.

Effect of CB loading

The effect on the mechanical properties of the nanocomposite caused by the variation in the loading of CB (HAF) from 30 to 50 phr, in steps of 10 phr, has been demonstrated in Figs. 1 and 2, which correspond to the nanoclay- and nanofiber-filled nanocomposites, respectively. N330-filled systems have been designated by (●) and the 'dash' line in both the figures. Comparison has been performed against the 50 phr HAF-containing sample (R-0/N3-50, control) because it is the conventional level of CB loading in commercial rubber products.

Clay-based nanocomposites

A comparison of properties of clay-based nanocomposites at different loadings of CB with those of the control composite (R-0/N3-50) is shown in Fig. 1. The graph in Fig. 1 illuminates the attainment of best set of properties (modulus at 300% elongation, TS, and TR) at 50 phr loading of N330, compared to those of the corresponding control composite, R-0/N3-50. In each of the graphs, the dotted line parallel to the abscissa represents the property of the R-0/N3-50 microcomposite (Figs. 1 and 2). Even

Table 2 Mechanical properties of NR gum and nanocomposites (both, nanoclay- and nanofiber-based) and those filled with HAF at 50 phr loading

Sl. No.	Sample	300% modulus (MPa)	TS (MPa)	EAB %	Tear (N/mm)	HLR first cycle	HBU (°C)
1	N	2.04	20.64	973	29.8	0.169	2
2	TiNSP4	3.18	28.20	963	36.1	0.386	3
3	BNF6	4.36	23.00	816	38.1	0.379	3
4	R-0/N3-50	9.19	22.05	573	46.9	0.436	5
5	NC-4/N3-50	12.15	25.15	526	55.4	0.492	6
6	NF-6/N3-50	12.85	23.45	482	54.5	0.536	6

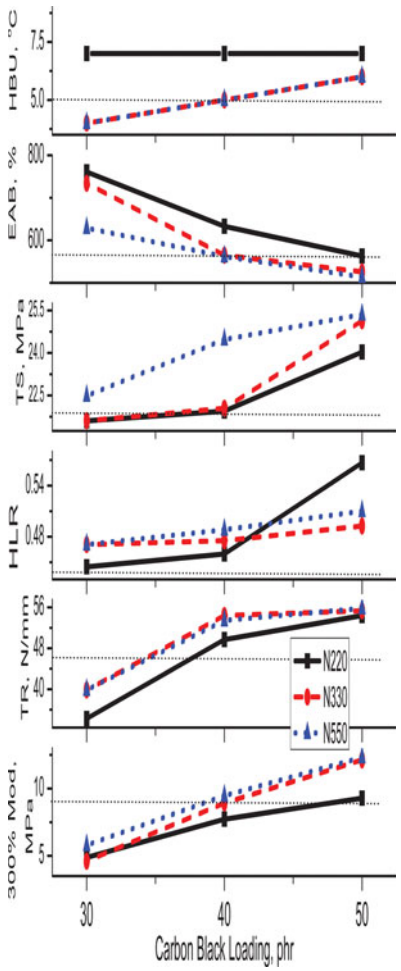

Fig. 1 Comparison of properties of nanoclay-based nanocomposites and those of control composite, at different filler loadings of three different CBs (where the *dotted line* corresponds to the control composite, R-0/N3-50)

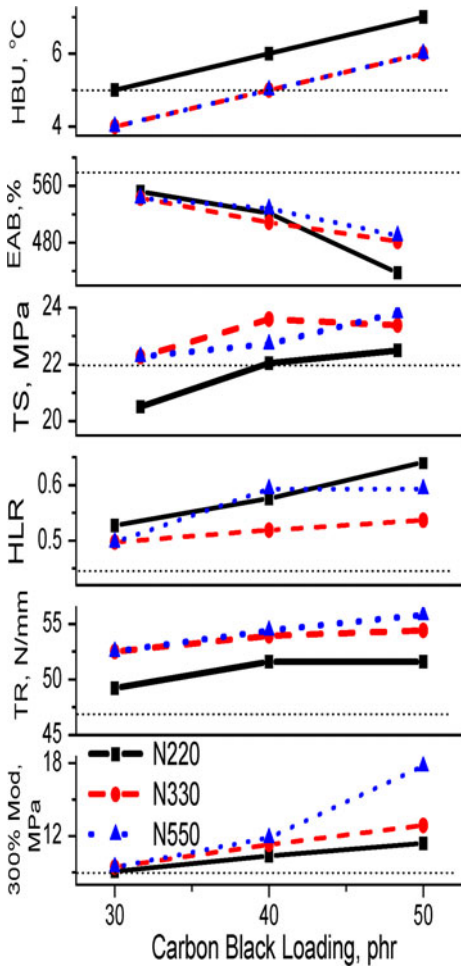

Fig. 2 Comparison of properties of CNF-based nanocomposites and those of the control composite, at different filler loadings of three different CBs (where the *dotted line* corresponds to the control composite, R-0/N3-50)

with lowering of CB loading by 10 phr, the improvement in tensile and tear strength over the 50 phr control composite (R-0/N3-50) is retained, as seen in Fig. 1. These also correspond to 182 and 50 % increment in the modulus and tear strength over the gum nanocomposite (TiNSP4). The already high tensile strength, which is the hallmark of the clay-containing nanocomposites, is affected a little adversely (see Table 2).

Both HLR and HBU increase with increase in filler loading from 30 to 50 phr (Fig. 1). In general, HBU increases with filler loading because of decrease in inter-filler particle distance, which causes frictional heat generation. Here, unit increment with every 10 phr loading is observed. More significant is the rise in HLR, which contributes favorably to the overall increase in tear strength, as observed earlier [18]. The EAB falls by around 30% because of the restricted mobility and the hindrance in slippage of the elastomer chains (Fig. 1).

CNF-based nanocomposites

The comparative study of properties of CNF nanocomposites and those of the control microcomposite (R-0/N3-50), at different filler loadings of CB, is illustrated in Fig. 2. In tandem with the nanoclay-filled system, almost all the properties studied are found to be better than those of the control microcomposite (Fig. 2) at all loadings of N330 in these carbon nanofiber (F)-based compounds. This is because of the favorable dispersion and association of the two fillers present in the matrix by virtue of their differences in zeta potential (ZP, discussed later). As the graphs in Fig. 2 show, the sustained effect of the nanofiber over black (R-0/N3-50) is best demonstrated at 50 phr loading. This particular loading corresponds to the best modulus at 300% elongation (40%) and tear strength (16%) property increment at moderate HLR values, when compared to their only black microcomposite counterpart (Fig. 2).

Owing to the presence of additional particulate matter in the 30, 40, and 50 phr HAF black-loaded nanocomposites, the modulus in CB-filled CNF nanocomposites enhances over the gum nanocomposites, by 117%, 159%, and 306%, respectively. Similarly, the tear strength, at all three loadings, registers increase of at least 32% over the nanocomposites devoid of CB (Fig. 2). However, such outstanding increments are achieved at the expense of slightly hysteretic compounds. Interestingly, unit temperature increase in HBU is recorded with every 10 phr of additional black loading, in accordance with the black-filled nanoclay systems. EAB decreases with CB loading, as in the case of clay-based nanocomposites.

It is worth mentioning here that in both the nanofiller (clay/CNF) systems, even a 10 phr lowering of CB loading does not impair material properties significantly. Particularly in the case of CNF systems, even 20 phr reduction in black loading can be afforded without making any significant compromises in the useful properties (Fig. 2). This is obvious form the fact that almost all the points are above the dotted line parallel to the X-axis. This line represents the corresponding property of the control.

Effect of type of CB and its loading

Having established the sustenance of property improvement in nanocomposites even in the presence of CB, it is imperative to study the effect of other grades of CB [N220 (■) and N550 (▲)]. N220 and N550-filled systems have been designated by the "continuous" line and the "short dash" line, respectively. The legends have been clearly defined in both the graphs, as well (Figs. 1, 2). These aspects are discussed in the following section.

Clay-based nanocomposites

In the case of clay nanocomposites, at 30 phr loading of the N220 and N550 black-filled NR samples, as expected, the properties fall way short of the R-0/N3-50 sample (Fig. 1). On increasing the loading by 10 phr, other properties in general are comparable to those of the base compound (R-0/N3-50). The lower modulus values can be attributed to the lesser number of particulate moieties in the matrix. In these compounds, the combined effect of improvement in TS and EAB ensure better ultimate properties than R-0/N3-50. It is noteworthy that the tear strength of these mixes is around 50% higher than that of the corresponding nanocomposites devoid of CB (TiNSP4).

At 50 phr loading of CB in the clay nanocomposites, similar trends are observed (Fig. 1). The best set of properties is shown by the N330 (HAF)-filled nanocomposites. Tensile and tear strength exhibit around 10–20% increment, compared to the base black mix of R-0/N3-50. The lower values for ISAF is primarily due to limited dispersion in presence of existing nanofillers, the ensuing restriction causes formation of localized clusters of CB (explained later). This is also reflected in the high HLR.

In general, with decrease in inter particle distance and filler loading, HBU increases due to frictional heat generation because of the breakdown in structure of blacks during cyclic testing. Since N220 is a high-structured black, HBU is higher for N220-filled samples than for N330 and N550-filled ones. HBU shows a near linear correspondence with CB loading for all the systems, except the N220-filled nanocomposites. Here, possibly due to the high surface area, N220 is already highly aggregated, even at 30 phr loading. Hence, no observable change in HBU was noted with CB loading (Fig. 1). The tensile strength and EAB do not depict any discernible change beyond the experimental errors.

CNF-based nanocomposites

Similar investigation has been carried out on the effect of CB type and loading on nanofiber systems (Fig. 2). At 50 phr loading, the observed values of the modulus at 300% elongation: 11.40, 12.85 and 17.69 MPa; and tear strength: 51.8, 54.5 and 53.8 N/mm for ISAF, HAF and FEF-filled NR/CNF nanocomposite, respectively. NF-6/N3-50 registers the highest tensile and tear strength values, which correspond, respectively, to 6 and 16% increments over R-0/N3-50. It also records 40% enhancement of modulus at 300% elongation. All these compounds demonstrate at least 160% enhancement in modulus at 300% elongation and 36% increment in tear strength over the CNF nanocomposite not having CB (BNF6).

It is interesting to note that in line with the observations in our earlier publication [17, 18], the presence of CNF raises the tear strength values beyond that of the base (R-0/N3-50), even in 30 and 40 phr CB loaded nanocomposites. HLR is found to steadily increase in presence of CNF, unlike nanoclay-filled systems where significant rise is observed only at high loadings (Figs. 1, 2). A close look at the HLR values again illustrates the close linear correspondence between tear strength and HLR, for each set of CB (Fig. 3). HBU shows linear correspondence with CB loading for all systems (Fig. 2). The tensile strength and EAB exhibit trends similar to the clay-based nanocomposites, as these properties do not depict any discernible change beyond the experimental errors.

Dynamic mechanical thermal analysis

The mechanical properties depicted the positive and sustained influence of the nanofillers, even in the presence of CB at high loadings, especially in HAF-filled samples. The

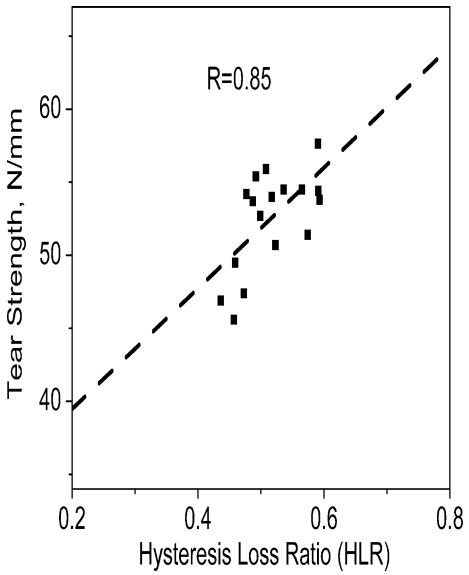

Fig. 3 Dependence of tear strength on hysteresis loss ratio

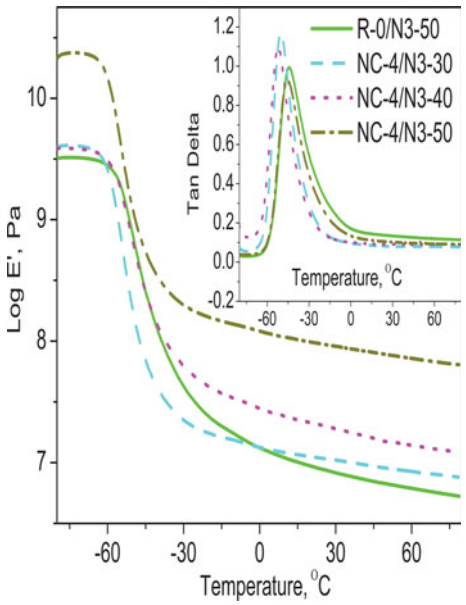

Fig. 4 Storage modulus and tan δ (*inset*) of NR, black microcomposite and clay-filled nanocomposite on incorporation of CB

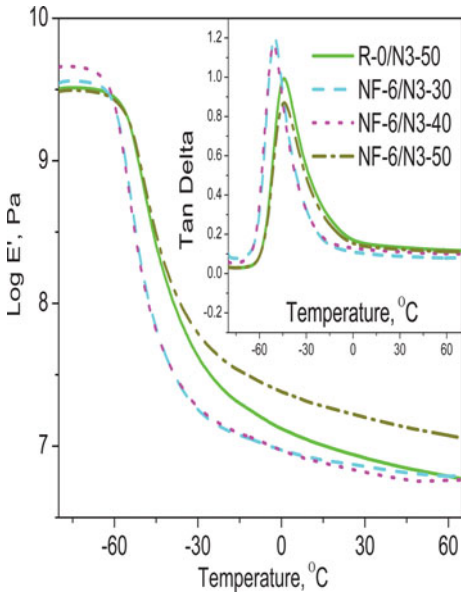

Fig. 5 Storage modulus and tan δ (*inset*) of NR, black microcomposite and CNF-filled nanocomposite on incorporation of CB

conformity of trends in mechanical and dynamic mechanical properties thus needs to be studied by investigating these systems for their dynamic mechanical properties. The dynamic mechanical behavior across a wide temperature range of the HAF-filled clay and nanofiber nanocomposites under small-amplitude oscillatory tensile strain is shown in Figs. 4 and 5, respectively, while the important properties are reported in Table 3.

On using HAF black, a phenomenal increase of storage modulus (at 25 °C) is recorded in the presence of nanoclay over the only black-filled control; for instance, the 50 phr HAF-filled sample, NC-4/N3-50, exhibits 326% increase over R-0/N3-50 (Table 3). As in the case of mechanical properties, with 130% increase, even the 40 phr loaded sample reflects the black-nanoclay synergy, while at 30 phr the changes are less significant (23%). Even the low temperature modulus increases with increasing stiffness of the sample due to the presence of dual filler system (Fig. 4). It was earlier demonstrated in Fig. 1 that the tensile strength and modulus also undergo similar drastic jumps with 10 phr increment in CB loading (Fig. 1). In this regard, comprehensive discussion substantiated by transmission electron micrographs has been provided in the succeeding morphology section. Similar observations are made for the CNF-containing black nanocomposites (Fig. 5). In this case, the 50 phr black sample exhibits outstanding improvement of 91% in the storage modulus at 25 °C.

These increments in storage modulus provide ample indication of the enhanced stiffness and restricted mobility, which also induces greater damping in these advanced composite materials. This is reflected in the viscous behavior of these dual filler systems measured in terms of the loss factor at T_g (Insets of Figs. 4, 5). The loss factor (tan δ) gives the fractional energy lost in a system due to deformation as heat.

At temperatures sufficiently lower than those corresponding to the tan δ_{max} molecular slippage and other motions are frozen. The resulting loss factor is small, since nearly all the energy stored in deforming the material is quickly recovered when the stress is removed. Inclusion of fillers, both nano (clay and fiber) and CB, changes the

Table 3 Representative dynamic mechanical properties of NR gum and nanocomposites (both, nanoclay- and nanofiber-based) filled with HAF black at different loadings

Sample	T_g	Tan δ_{max}	% Change in tan δ at T_g	Tan δ at 0 °C	Tan δ at 60 °C	% Change in tan δ at 60 °C	Storage mod. at 25 °C (MPa)	% Increase in modulus at 25 °C
R-0/N3-50	−44	0.99	0	0.16	0.12	0	8.81	0
NC-4/N3-30	−50	1.16	17	0.10	0.08	−33	10.84	23
NC-4/N3-40	−48	1.09	10	0.13	0.09	−22	20.23	130
NC-4/N3-50	−50	0.92	−7	0.14	0.09	−24	37.49	326
NF-6/N3-30	−51	1.20	21	0.11	0.08	−34	7.47	−15
NF-6/N3-40	−51	1.17	18	0.13	0.10	−15	6.89	−22
NF-6/N3-50	−44	0.87	−12	0.15	0.11	−6	16.86	91

damping behavior of the polymer; the most pronounced effects being the lowering of loss factor at 60 °C temperature, T_g (upto 34%) and the broadening of the transition peak. The only black-filled NR system has a loss factor of 0.99 at the T_g; the presence of either nanoclay or nanofiber reduces the loss factor by around 10% for the 50-phr-loaded samples (Table 3). At lower black loadings, such decrements are obviously not observed. Widening of the tan δ curve at the glass transition region is observed because of the adsorption of the polymer on to the fillers, which restricts segmental motion of molecular chains in the neighborhood of the restraining surface. The presence of CNF and organomodifier in clay induces a lubricative effect thereby increasing the low temperature mobility and causing a concomitant decrease in T_g (the temperature corresponding to tan δ maximum). However, these CB-filled nanocomposites possess much higher T_g than those observed in our earlier publication [18], for pure rubber or modified nanoclay/nanofiber systems. In these nanocomposites, the rubber molecules have reduced chain mobility as the reinforcing effect of the various fillers dominates, by virtue of the strong interfacial action between the rubber matrix and the nanofiller–filler associations. Also, it has been reported earlier that if T_g is less than −60 °C, wet grip becomes inferior and, if it exceeds −40 °C, rolling resistance becomes inferior [23]; all the compounds designed here lie within this high performance window.

Tan δ values at 0 and 60 °C, represent the wet skid and rolling resistance, respectively of rubber compounds employed in tire applications. It is desirable to have high loss factor at 0 °C to achieve necessary wet traction and grip. On the other hand, low loss factor at 60 °C ensures lesser fuel consumption and lesser emissions and lower carbon footprint. It can be clearly seen in Table 3, that the clay-black nanocomposites, in particular, show the best mix of dynamic mechanical properties of high storage modulus, and tan δ at 0 °C along with significantly low rolling resistance. As discussed in the introductory section, such properties may render these nanocomposites suitable for use in tire tread compounds. The advantages of the dual filler system over the controlled CB in rubber performance is evidenced by the higher tensile, tear, modulus, EABand desirable tan δ than the only black-filled composite.

Morphology–property relationships

The TEM images shown in Fig. 6 are the representative images of the nanocomposites studied to comprehend the morphology developed in nanoclay and nanofiber-based systems in the presence of CB. Three-phase morphology is evident in the TEM micrographs (Fig. 6a–f): the nanoclay (Fig. 6a–c) and nanofiber (Fig. 6d–f) appear as dark striations, the CB as dark gray circular blocks, aggregated in clusters and the representation of the rubber matrix is in light gray/white color.

TEM images show individual silicate layers with an aspect ratio in the range of 100–300 (Fig. 6a–c). The CNFs in the nanocomposite have average diameter of 130 nm, as compared to 77 nm in the supplied material (Fig. 6d–f). This swelling of the fiber by the percolation of rubber inside the hollow structure and formation of an envelope around the sheath is consistent with our previous observations [17, 18].

The nanofillers generally tend to orient parallel along the flow direction. However, a certain degree of isotropicity is observed in these nanocomposites. This characteristic can be attributed to the fact that the rubber band is regularly cut at 45° and folded over meticulously to obviate the effects of anisotropy. This renders the flow direction less consequential. The overbearing presence of CB acts as a guide pin for nanofiller orientation as they are found trapped between the black clusters forming “nano-blocks”. Owing to the strong intermolecular interactions between nanofiller/NR/black, a ternary hybrid structure, designated as “nano-blocks”, are found to form across the matrix. These are indicated in Fig. 6a, c and d, e by arrows. Similar observations, attributed to surface activity and charge, have earlier been reported with clay and black, and titania and

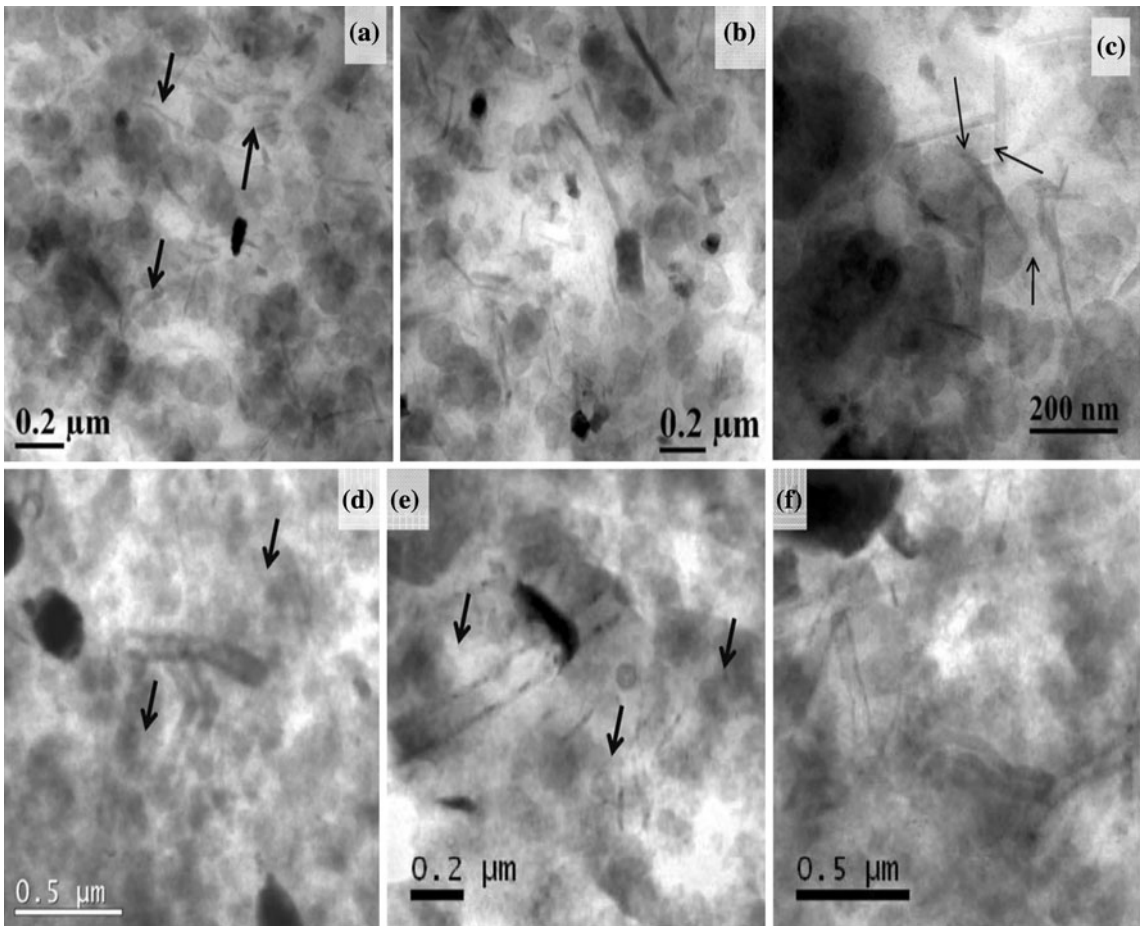

Fig. 6 TEM pictures of CB-filled nanocomposites in the presence of **a–c** sepiolite modified with dispersion techniques and **d–f** CNF nanocomposites post process-modification systems at optimized loading; where the *dark spherical areas* represent the CB aggregate, the *dark layers* represent the clay nanoplatelet, and the *gray/white areas* represent the NR matrix

carbon nanotube filler systems [24–26]. Black aggregates preferably get aligned within the passages between such "nano-blocks" forming a network structure which enables efficient stress and heat transfer from the matrix (Fig. 6a, b, d, e). These passages (Scheme 2) have earlier been designated as "nano-channels" [24]. Local nanofiller orientation in relatively black-free regions, on the other hand, shows random orientation (Fig. 6c, f).

In order to garner a comprehensive understanding of the microstructure developed in these dual filler systems, the concept and literature values of ZP have been employed here. Zeta potential (ZP) is a measure of surface charge, and previous studies on adsorption have explicitly demonstrated that the ZPs of the nanofillers at pH levels encountered in rubber mixes are negative, while those of CBs used for our investigation are positive [27–31]. ZP has been utilized here merely as a tool to represent the charges on the nanofillers which are otherwise difficult to measure real time in such complicated elastomer systems. It must be mentioned here that ZP is not only applicable to aqueous systems, but also to highly viscous non aqueous fluids, for e.g., polymer melts. For instance, Brochartd-Wyart and de Gennes [32] and Flores et al. [33] have studied ionic diffusion of ultrafine particles in polymer melts. Nanosilica stability in poly(ethylene glycol) melts using conductance studies have also been performed as a tool to determine the second virial coefficient [34]. Also, the black–clay bonhomie in similar melt mixed polymer nanocomposites have been earlier reported by Konishi and Cakmak [25], and Feller et al. [35].

The as-grown and acid-treated CNFs are negatively charged in the entire pH range up to 12 [27], Sabah et al. [28] found smectite clays to possess negative ZP, Gates [29] found sepiolite to have their ZPs at around −18 mV over the pH range from 2 to 11 [30], while Xu et al. observed polydisperse agglomerates existed for CB in non-polar media, which resulted in ZPs of around +20.8 mV in toluene [31]. Since CB has positive ZP, it is only obvious that the negatively charged nanoparticles (sepiolite and CNF) get attracted to the positively charged black surface, rendering stability to the microstructure thus formed. Nanocomposite properties are known to have improved by

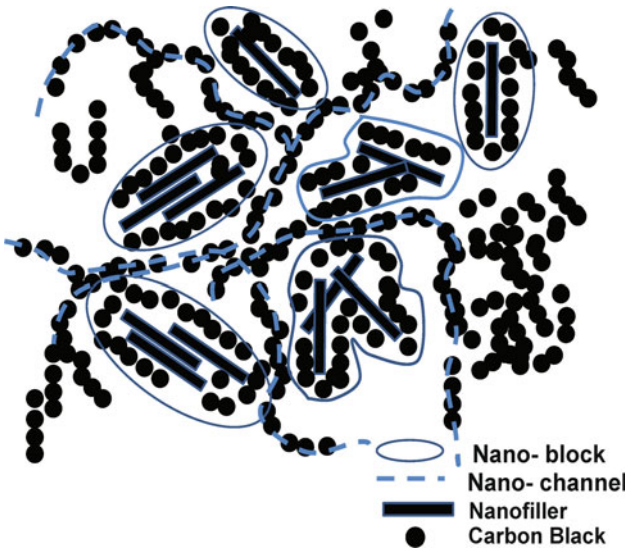

Scheme 2 Microstructural development in nanoclay and nanofiber-based nanocomposites in the presence of CB

formation of close associations of CB-clay moieties (i.e., haloing) during processing, where the clay exists in a non-exfoliated state and is surrounded by CB clusters [24]. Anionic clays and negatively charged surfactants are known to exhibit tremendous affinity toward carbonaceous fillers [36]. Such specific microstructure development because of nanofiller associations by virtue of favorable ZP disposition had earlier been identified [37] and applied to polymer nanocomposites too [24]. Grunlan and coworker found that the liquid state dispersion through synergistic stabilization was largely retained even in the solid matrix. Similarly, here during mixing under high temperature and shear, the rubber stays in a liquid state and solidifies only after curing during molding. In such a viscous liquid state, close correspondence may be expected and the ZP driven associations might play important role. Such restrictions are also aided by stronger nanofiller–CB interaction in comparison to CB–rubber interaction. Similar observations were made for clay/CB in poly(ethylene), poly(propylene) and poly(ethylene-coethyl acrylate) [35] and clay/SWNT in epoxy [38].

Therefore, electrostatic interactions between the nanoparticles (sepiolite/nanofiber) and CB explains the formation of the hybrid ternary "nano-blocks", which further assists their dispersion in the matrix. The attachment of sepiolite/nanofiber at the surface of CBs weakens the electrostatic interactions between CB particles due to reduction in free surface area, thereby preventing their re-agglomeration during curing, as well.

By virtue of such electrostatic interactions, there exist two types of CB particles in these nanocomposites, one in close proximity of nanofiller (clay/nanofiber) and the other in aggregates of other CB particles. The former has been earlier referred to as "associated CB" (shown in Scheme 2 and referred to as "nano-blocks") and the latter as "free CB" [24]. It is the distribution of these free CB in the presence of nanofillers that leads to the formation of efficient networks because of the formation of "nano-channels". These channels are networks of free CB particles that connect the associated CB leading to pathways for heat and stress transfer. This has been schematically shown in Scheme 2, which illustrates the microstructure developed in the presence of adequately dispersed dual filler systems. The efficiency of stress transfer is dependent on the formation of "nano-blocks", "nano-channels", and the size of CB aggregates termed here as "free CB".

The different observations made during this study can be explained in view of the above morphological insight. For instance, in the case of the composite containing only CB (R-0/N3-50; control), large aggregates (>1.5 μm diameter) are randomly dispersed in the matrix, which result in early saturation of properties. On the other hand, in most of the nanocomposites containing CB there exist networks of aggregates of relatively smaller size ($\sim$ 240-nm diameter), along with a favorable disposition of "nano-blocks". This accounts for their much enhanced properties.

In the case of clay nanocomposites, at 30 phr loading of N220 and N550 black-filled samples, the properties fall way short of the R-0/N3-50 control sample (Fig. 1). This is because they contain much less free CB than that required for the establishment of a network structure of small-sized aggregates. The trend in properties of CB-filled composites thus changes in the presence of nanofillers. Furthermore, N220 by virtue of its large surface area and activity possesses highly positive ZP and thus has a tendency to self-assemble into in large clusters where nanofillers get entrapped. It renders them unavailable for interaction with the rubber. This not only limits the inter-particle distance thereby increasing the filler–filler interactions, but also results in poor overall properties because of insufficient rubber–filler interaction necessary for reinforcement. This is corroborated by the mechanical property data (Fig. 1). As with other nanofillers having exceedingly high surface area, it is difficult to adequately disperse N220 at high loadings. It forms big aggregates, thereby failing to impart any beneficial effect on the matrix properties in terms of reinforcement. This is in agreement with the observations made earlier by other authors [24] who had noted that even in the presence of nanofillers, only small-sized CB aggregates could favorably impact the mechanical strength, albeit at the expense of electrical conductivity.

Enhancement in properties is not only dependent on the surface area of the nanofiller. It is in fact a function of surface area and loading, as well. Based on the polymer–filler combination, beyond a certain critical loading, increase in surface area has a detrimental effect on the

properties. This is attributed to the decrease in the actual surface area available for interaction with the polymer because of filler aggregation tendencies. Such aggregation tendencies can be overcome by modifying the nanofillers or tweaking the filler incorporation process. For instance, unmodified MMT has large surface area, but it also possesses high cleavage energy because of which individual platelets cannot be dissociated easily from the stacks. Bhowmick et al. have demonstrated through extensive HRTEM image and statistical analysis that water-assisted mixing of Cloisite-Na+ (Na-MMT) opens up larger amount of clay surface area for interaction with NR [39]. They found that Na-MMT can be dispersed in NR latex and subsequently mixed with the other ingredients by conventional mixing process to exfoliate the unmodified nanoclay. Direct melt mixing of NR/Na-MMT had earlier been found to be ineffective in dissociating the firm aggregates of unmodified clay, although it could exfoliate organomodified clays to much greater extents [18].

The 50-phr-CB-loaded clay-filled samples possibly show the best mix of free and clay-aggregated CB leading to the formation of appropriate "nano-channels" for stress transfer (Figs. 1, 4). The sepiolite clay acting as a dispersing agent for CB is able to form a network structure of small aggregates. This is reflected in terms of the superior mechanical properties (Fig. 1) and especially the remarkably high room temperature storage modulus (Fig. 4). Similar behavior is demonstrated by the CNF systems (Figs. 2, 5), which also possess negative ZP in the pH environment existent in such rubber compounds. Possibly because of the higher magnitudes of such charges, in comparison with sepiolite, they can form "nano-blocks" and "nano-channels" more efficiently. Thus, they can establish strong supramolecular filler networks (Scheme 2) required for stress and heat transfer, even at 30 phr loading. Stronger networks are built on increasing the CB loading up to 50 phr. Such networks of small aggregates, with large surface area for rubber–filler interaction, are known to perform better in terms of reinforcement.

In the nanocomposites, the ease of transferring applied stresses from the matrix onto the nanoparticles, due to the very high surface area available for rubber–filler interaction, results in an enhancement of the physico-mechanical properties. Also, the compatibilizer (in clay-based systems) breaks up the agglomerates of the nanoparticles into finer particles, enhancing their degree of dispersion in the elastomeric matrix by increasing the interfacial adhesion. In the CB-containing nanocomposites, the nanofillers act as dispersing agent, as well. They help disintegrate the large CB aggregates and render stability to the dispersion of small aggregates by the formation of nano-blocks and channels. The much enhanced properties in highly filled black samples are primarily due to the attainment of such unique ternary filler arrangements, discussed above. This ternary arrangement comprising the stand-alone nanofiller, CB moieties, and distinctive nano-blocks is formed from the preferential association of CBs and nanofillers. The beneficial effect of such ZP-driven associations (nano-blocks), in terms of efficient stress transfer and heat dissipation, have earlier been illustrated [24, 25]. Nanofiller dispersion, randomized and isotropic, remains largely unaltered even in the presence of CB because of the repeated cutting and folding over of the rubber bands during open roll mixing.

These novel congregations thus provide the platform for homogenous distribution of the nanoparticles in the form of nano-blocks and channels. Such spatial distributions of the hybrid structures ensure efficient stress transfer and arrest sub-surface crack growth propagation. As a result, there is concomitant enhancement in the tensile, dynamic, mechanical, and abrasion properties even in the overbearing presence of CB.

Conclusions

NR-based nanocomposites—categorized into two types: the nanoclay filled and nanofiber filled—have been prepared by suitable dispersion techniques and studied separately. Subsequently, they have been mixed with various furnace blacks in an internal mixer to form clay/CB and CNF/CB nanocomposites. Their tensile, tear, hysteresis loss, and heat buildup (HBU) properties have been extensively studied. TEM and dynamic mechanical analysis of some representative samples also have been performed.

HAF carbon black provided the best set of properties (modulus at 300% elongation, TS, and TR), even in the presence of nanofillers, due to its exquisite balance of surface area, structure and surface activity. Ternary filler architecture was observed because of formation of a unique microstructure comprised of "nano-blocks", small size aggregates of CB, and "nano-channels" of free CB. These blocks, formed from favorable electrostatic interactions induce enhanced filler dispersion and efficient stress transfer from the matrix, resulting in improved mechanical and dynamic mechanical properties, not only in the overbearing presence of CB but also on significantly reducing the black loading. These nanocomposites exhibit an increment of 18% in tear strength, 40% in modulus at 300% elongation, and 326% in storage modulus, over the control microcomposite. The location of T_g within the high performance window in the range from −60 to −40 °C, along with low loss factor values at 60 °C, ensures that demanding requirements of modern day application in terms of strong mechanical strength in conjunction with low rolling resistance could be met, without compromising

on the wet grip resistance. These are rendered possible by virtue of the black/nanofiller synergy. The results could be explained by ZP driven morphological dispositions, corroborated by TEM.

By virtue of the synergistic effect, with the two fillers benefitting from each other, NR nanocomposites containing dual fillers showed remarkable improvement as well over both the CB-filled microcomposites and the nanocomposites devoid of CB.

References

1. Kojima Y, Usuki A, Kawasumi M, Okada A, Kurauchi T, Kamigaito O (1993) J Appl Polym Sci 49:1259
2. Messersmith PB, Giannelis EP (1995) J Polym Sci Part A: Polym Chem 33:1047
3. Gonsalves K, Chen Y (1996) Mater Res Soc Symp Proc 435:55
4. Usuki A, Kawasumi M, Kojima Y, Okada A, Kurauchi T, Kamigaito O (1993) J Mater Res 8:1174
5. Okada A, Kojima Y, Kawasumi M, Fukushima Y, Kurauchi T, Kamigaito O (1993) J Mater Res 8:1179
6. Giannelis EP (1996) Adv Mater 8:29
7. Ray SS, Okamoto M (2003) Prog Polym Sci 28:1539
8. Utracki LA, Sepehr M, Boccaleri E (2007) Polym Adv Technol 18:1
9. Maiti M, Bhattacharya M, Bhowmick AK (2008) Rubb Chem Technol 81:384
10. Iijima S (1991) Nature 354:56
11. Ajayan PM, Schadler LS (2001) Polym Prep 42:35
12. Barrera E (2000) JOM 52:38
13. Burton DJ, Glasgow DG, Lake ML, Kwag C, Finegan JC (2001) Proceedings of the 46th international SAMPE symposium and exhibition: materials and processes odyssey, California, USA
14. Kumar S, Doshi H, Srinivasaro M, Park JO, Schiraldi DA (2002) Polymer 43:1701
15. Lozano K (2000) JOM 52:34
16. Carneiro OS, Maia JM (2000) Polym Compos 21:960
17. Bhattacharya M, Maiti M, Bhowmick AK (2008) Polym Eng Sci 49:81
18. Bhattacharya M, Maiti M, Bhowmick AK (2008) Rubb Chem Technol 81:782
19. Donnet JB, Voet A (1976) CB: physics, chemistry, and elastomer reinforc. Dekker, New York
20. Wolff S (1996) Rubb Chem Technol 69(3):325
21. Maiti M, Sadhu S, Bhowmick AK (2005) J Appl Polym Sci 96:443
22. Jia QX, Wu YP, Ping X, Xin Y, Wang YQ, Zhang LQ (2005) Polym Polym Comp 13:709
23. European Patent: EP0500338 (A1) (1992) Inventor(s): Yuichi S, Susumu W, Sumio T, For Sumitomo Rubber Ind
24. Etika KC, Liu L, Hess LA, Grunlan JC (2009) Carbon 47:3128
25. Konishi Y, Cakmak M (2005) Polymer 46:4811
26. Sumfleth J, Prado LASA, Sriyai M, Schulte K (2008) Polymer 49:5105
27. Kvandea I, Øyeb G, Hammera N, Rønninga M, Raaenc S, Holmena A, Sjöblomb J, Chen D (2008) Carbon 46:759
28. Sabah E, Mart U, Çnar M, Çelik MS (2007) Sep Sci Technol 42:2275
29. Gates WP (2004) Appl Clay Sci 27:1
30. Lin JJ, Chu CC, Chiang ML, Tsai WC (2006) J Phys Chem B110(37):18115
31. Xu R, Wu C, Xu H (2007) Carbon 45:2806
32. Brochard-Wyart F, de Gennes P (2000) Eur Phys J E 1:93
33. Flores F, Graebling D, Allal A, Guerret-Pi'ecourt C (2007) J Phys D Appl Phys 40:2911
34. Anderson BJ, Zukoski CF (2007) Macromolecules 40:5133
35. Feller JF, Bruzaud S, Grohens Y (2004) Mater Lett 58:739
36. Moore VC, Strano MS, Haroz EH, Hauge RH, Smalley RE, Schmidt J, Talmon Y (2003) Nano Lett 3:1379
37. Tohver V, Smay JE, Braem A, Braun PV, Lewis JA (2001) Proc Natl Acad Sci USA 98:8950
38. Liu L, Grunlan JC (2007) Adv Funct Mater 17:2343
39. Bhowmick AK, Bhattacharya M, Mitra S (2009) Paper # 103 at the 176th fall technical meeting of Rubber Division, ACS, 14th October 2009, Pittsburgh, USA